Article:
Forster, Piers M., Forster, Harriet I., Evans, Mat J. orcid.org/0000-0003-4775-032X et al. (11 more authors) (2020) Current and future global climate impacts resulting from COVID-19. Nature Climate Change. 913–919. ISSN 1758-678X

https://doi.org/10.1038/s41558-020-0883-0

Current and future global climate impacts resulting from COVID-19

Piers M. Forster (1), Harriet I. Forster (2), Mat J. Evans (3,4), Matthew J. Gidden (5,12), Chris D. Jones (6), Christoph A. Keller (7,8), Robin Lamboll (9), Corinne Le Quéré (10,11), Joeri Rogelj (9,12), Deborah Rosen (1), Carl-Friedrich Schleussner (5,13), Thomas B. Richardson (1), Christopher J. Smith (1,12), Steven T. Turnock (1,6)

1. Priestley International Centre for Climate, University of Leeds, UK (p.m.forster@leeds.ac.uk)
2. Queen Margaret's School, Escrick, York, UK
3. Wolfson Atmospheric Chemistry Laboratories, Department of Chemistry, University of York, York, YO10 5DD, UK
4. National Centre for Atmospheric Science, University of York, York, YO10 5DD, UK
5. Climate Analytics, Berlin, Germany
6. Met Office Hadley Centre, Exeter, UK
7. NASA Global Modeling and Assimilation Office, Goddard Space Flight Center, Greenbelt, MD, USA
8. Universities Space Research Association, Columbia, MD, USA
9. Grantham Institute for Climate Change and the Environment, Imperial College London, UK
10. School of Environmental Sciences, University of East Anglia, UK
11. Tyndall Centre for Climate Change Research, University of East Anglia, UK
12. Energy Program, International Institute for Applied Systems Analysis, Laxenburg, Austria
13. IRI THESys, Humboldt University, Berlin, Germany

Abstract

The global response to the COVID-19 pandemic has led to a sudden reduction of both greenhouse gas emissions and air pollutants [1–3]. We use the unprecedented access to national mobility data [4,5] to make a bottom-up estimate of global emission reductions for February-May 2020. The resulting NOx trends agree well with meteorologically-adjusted surface based NO_2 observations. In our upper bound estimate, global NOx emissions have declined by over 25%, resulting in a negative radiative forcing trend and short-term cooling since the start of the year. This cooling trend is offset by a ~20% reduction in global SO_2 emissions, that weakens the aerosol cooling effect, causing short-term warming. Over the next ten years, the competing warming and cooling effects of these non-CO_2 emission changes more or less cancel, giving a time varying overall cooling compared to a baseline scenario that doesn't include the COVID-19 dip, similar to the CO_2 only temperature response. We estimate this direct effect of the pandemic driven response will be negligible, with a cooling of around 0.01 ± 0.005 °C by 2030 compared to a baseline scenario which follows current national policies. In contrast, with an economic recovery tilted towards green stimulus and reductions in fossil fuel investments, we can avoid a future warming of 0.3°C by 2050 and have a greater than 50% chance of limiting the increase in global surface temperature to 1.5°C above pre-industrial levels.

Key findings:

- The direct effect on the global surface temperature over the next 10 years will be small even with a sustained 2-year lockdown period, but the long-term effect doesn't have to be. There is potential to limit global warming to 1.5°C, if lessons are learned from COVID-19 and changes are made towards more sustainable emissions reductions.

- Declines in SO_2 emissions from the power and industry sectors are calculated to be currently causing a short-term warming. These are being offset by the cooling due to the 25% decline in NOx emissions from surface transport reductions. This suggests that policies directed at limiting pollution from road transport could offset the short-term warming that results from policies which reduce pollution from the power sector.
- Aerosol forcing and tropospheric ozone forcing are not well enough known to determine the sign of temperature change from now until 2025. However, we can be more certain that after 2025, the current emission reductions will mean that future temperature increases will be slightly smaller than they would otherwise have been without the COVID-19 lockdown.
- We use the unprecedented access to Google mobility data to estimate near real-time national emission trends for surface transport, residential, industry, commercial and power sectors. We find our estimates correlate well with national CO_2 emissions estimates from complementary approaches but our data gives higher changes for the non-transport sectors. We use this new approach to provide high-end emission reduction estimates.
- We use our new approach to make an upper-bound estimate of changes in CO_2 emissions and 9 further species, covering 123 countries and 99% of global CO_2 emissions. We ground-truth our estimates in 32 countries with meteorologically-corrected surface NO_2 observations.
- Researchers will need to look for a climate signature of the COVID-19 response in regional signals as the global temperature signal will likely be small.

1. Introduction

By the time the World Health Organization declared COVID-19 (scientifically referred to as the severe acute respiratory syndrome–coronavirus 2 or SARS-CoV-2) a pandemic on 11 March 2020, the virus had already spread from China, to other Asian countries, Europe and the US. As of 24 May 2020, cases have been identified in 188 countries or regions[6]. This has led to unprecedented enforced and voluntary restrictions on travel and work. Analysis of Google and Apple mobility data shows mobility declined by 10% or more during April 2020 in all but one of the 125 nations tracked. Mobility declined by 80% in five or more nations (Figure S1). Associated declines in air pollution have been observed from satellite data and from local ground based observations[7,8]. The large pollution declines are expected to be temporary as pollution levels are already returning to near normal levels in parts of Asia[9,10].

In this work we build a high-end estimate of emission changes in greenhouse gases and air pollution due to the COVID-19 global restrictions over February-May 2020 and project these into the future. We then use these emission changes to make a prediction of the resultant global temperature response. We examine the temperature response of a direct recovery to pre-COVID-19 national policies and emission levels, and also explore responses where the economic recovery to COVID-19 is driven by either a green stimulus package or an increase in fossil fuel use.

2. Emission trends

Bottom-up emission trend analyses have traditionally relied on a laborious collection of various energy industry related indicators and statistics from multiple sources[11]. The unprecedented recent access to global mobility data from Google and Apple gives a unique opportunity to compare trends across many countries with a consistent approach. We use their data to develop a new method of emission trend analysis. The advantage over previous approaches is the possibility of near real time analysis, national granularity and a systematic consistent approach across nations and over time. The disadvantages are that we lose the direct connection between energy and emissions and need to make assumptions about

these relationships. There are also disadvantages over the short time history of the mobility data and opacity from the data providers around their detailed methodologies and uncertainties. In this paper we make a simple set of assumptions to deduce emissions change estimates from this mobility data and test the new emissions change estimates extensively against the approach of Le Quéré et al.(ref. [2]).

Google and Apple mobility changes and the Le Quéré et al. data all indicate that over 50% of the world's population reduced travel by over 50% during April 2020 (Figure 1a). Google mobility trends indicate that over 80% of the population in the 114 countries in their dataset (4 billion people) reduced their travel by more than 50%. Google mobility data and emission reduction estimates based on confinement level analysis in Le Quéré et al. agree on country level surface transport trends to within ~20% (Figures 1b and S1). When we examine the trends for the countries that we expect have contributed most to the overall transport emission change (e.g. USA, European nations and India), good agreement between the datasets is observed, and their trends are well correlated in time (see Figure 1b and Figure S2). Workplace, retail and residential movement data from Google also map relatively well with corresponding industry, public and residential sector emission changes but only if the high estimate of the emission change in the Le Quéré et al. dataset (Figures 1b, 1c and S2) is employed.

Employing mobility data outside of the transport sector is likely to overestimate the emission change and this appears to be the case for CO_2 emissions when compared to two previous estimates [1,2]. Nevertheless, our national and US state level mobility-derived emission estimates are well correlated in time with emission changes from the Le Quéré et al. study (see examples in Figure S2). For the industry sector, differences may be due to the fact that the emissions from industrial activity are less correlated with mobility trends, due to automated machinery, inertia in closing operations, or alternative modes of work or a base-line level of industrial emission from heavy industry in the absence of production, neither which would be captured by the Google mobility data which only reports changes in phone locations. For the residential sector, the 20% median increase matches the UK smart meter analysis by Octopus Energy for the situation when previously empty houses were occupied during the day after lockdown restrictions began[12]. However, many households were already occupied during the day and in these situations when an additional occupant was added, energy use only increased by 4%. These factors likely mean that our Google-based trends overestimate the emission change from these sectors, leading to our Google based total emission trend estimate agreeing better with the high level emission estimate from the Le Quéré et al. dataset (compare datasets in Figure 1c). There is also a question about how representative the Apple and Google datasets are of wider national behaviour and how the use and penetration of these phone operating systems varies across regions[13]. For example, the over 80% drop in Apple driving mobility in India (Figure 1a and S1), may only represent the part of the population that are able to work from home. Therefore, the emissions trends in our work which are largely derived from Google mobility data, should be taken as a high estimate of the COVID-19 emission driven change (see methods).

In the following we construct 2020 emission changes largely from Google mobility data to estimate emissions changes from the restriction measures in response to the COVID-19 virus, as illustrated in Figure 1c. As Google data is not available everywhere, we employ the Le Quéré et al. analysis to cover important missing countries, in particular, China, Russia and Iran which are all large emitters whose citizens have been under significant restrictions related to COVID-19. We also use Le Quéré et al. data to provide additional trend estimates from aviation and shipping sectors (see methods).

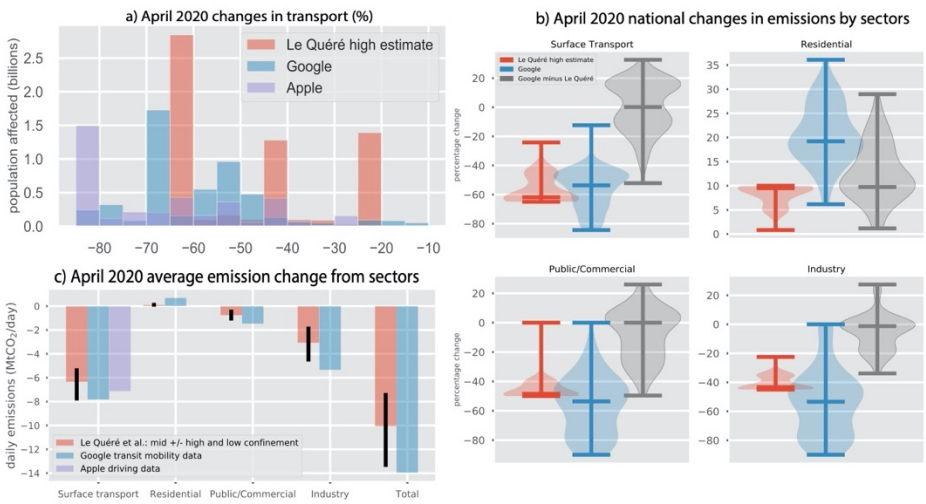

Figure 1. Comparison of sector emission trends. a) Population weighted histogram of surface transport trends from Apple driving data, Google transit data and Le Quéré et al. high confinement level data for available countries in the different datasets averaged over April 2020. b) Violin plots showing the distribution and maximum and median levels of national trends weighted by CO_2 emissions for the Google and Le Quéré datasets and the differences between the datasets evaluated over April 2020. c) Estimates of emission changes for the three datasets across four sectors for April 2020 and the sum of the four sectors. In Figures 1b and 1c data is shown for 60 countries with overlapping data in the Google and Le Quéré datasets (representing 60% of global CO_2 emissions). In Figure 1c, Apple data are for 57 countries, covering 58% of the global emissions. The high-confinement Le Quéré et al. data is used throughout, except in Figure 1c, where other confinement levels are shown for comparison as the range of the error bar on the mid-confinement level.

Our bottom up analysis uses 123 countries covering over 99% of global CO_2 emissions, extending the 69 countries analysed in Le Quéré et al. Daily national emission trends in six sectors are analysed for January-May 2020 (surface transport, residential, power, industry, public, and aviation). These are then weighted by the national and sector split of seven emitted species covering the major greenhouse gases and short-lived pollutants. National and sector data are taken from the Emissions Database for Global Atmospheric Research (EDGAR) version 5.0 database for 2015[14]. These data are combined to generate national and globally averaged daily emission changes in 2020 by species and sector.

In order to assess changes due to the COVID-19 pandemic, we establish a baseline scenario. We take a central estimate of emissions pathways[15], in which countries are assumed to meet their stated Nationally Determined Contributions (NDCs) by 2030. In this baseline, no further strengthening of climate action after 2030 is assumed to take place. To derive changes from this scenario a three-stage process is followed (see methods). First, fractional Google mobility data employs the 5-week period (Jan 3–Feb 6, 2020) as reference. Absolute emission trends are then computed by multiplying these fractional changes by either the 2019 CO_2 emissions from Le Quéré et al.[2] or, for other species, the 2015 emissions in the EDGAR database[14]. Finally these absolute changes are then applied to a steadily rising emission pathway based on pre-COVID national pledges (see Table 1). Only the globally average emission changes are used in this paper (see Figure 2a), but national and spatially gridded data are made available at https://github.com/Priestley-Centre/COVID19_emissions for other interested researchers.

Our analysis shows that emission reductions likely peaked in mid-April 2020 and that these reductions are species dependent. The data suggests that global CO_2 and NOx emissions could have decreased by

over 25% in April 2020 driven by a decline in transport emissions (Figures 2a, 2b and S3). Whereas, organic carbon (OC) has increased by <1% as it is primarily affected by rising residential emissions (Figures 2b and S3). Methane changes are driven by power sector declines, SO_2 is most strongly affected by declining industrial emissions. Generally, changes in surface transport are the biggest driver of change for most species analysed (Figure S3).

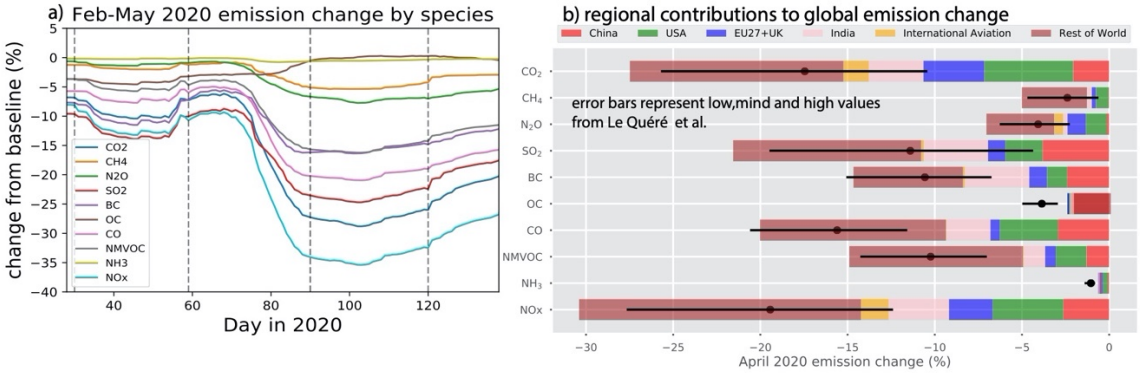

Figure 2. a) Percentage globally averaged emission changes for the considered species as a function of day in the year of 2020. b) A breakdown of the April 2020 average global emission reductions compared to a recent year for the different species. The breakdown is for major emission-nations, including international aviation. Global percentage emission changes from the baseline are shown on the x-axis (see details in Figure S4). Trends are relative to 2019 for CO_2, for the other species they are relative to 2015. The low, mid and high estimates of the total changes based on Le Quéré et al. trends are shown for comparison as the black circles and error bars.

Our data suggests that changes in emissions are not confined to the major emitting countries, the mobility restrictions have been of worldwide proportions (despite the extent of measures – and therefore relative emissions changes – varying globally) during April 2020 (Figure 1and S1), and this manifests itself in many countries contributing to the emission decline. For the short-lived species, Europe and the United States, in spite of their large fractional national emission change, make up a small percentage of the global response due their relatively low levels of emissions from pollution (Figure 2c and S4).

3. Observational evidence

Detecting a COVID-19 related signal in CO_2 concentrations is challenging due to CO_2's long atmospheric lifetime which makes any perturbation small. While the airborne fraction of CO_2 emissions is approximately 50% on multi-annual timescales[11], the airborne fraction of emissions changes is likely above 90% on sub-annual timescales[16,17]. Because CO_2 is not well mixed on the timescale of weeks to months, individual observing stations will not reflect the global CO_2 burden – for example Mauna Loa in the Northern hemisphere Pacific Ocean may see a larger signal than at the South Pole from the emissions reductions due to COVID-19 restrictions. The magnitude of natural – terrestrial and marine – fluxes of CO_2 compared with anthropogenic emissions make it extremely difficult to detect changes in emissions at national level from CO_2 concentrations themselves. We estimate these CO_2 concentration changes in Section 4 (see Figures S6 and 5b) and find maximum reductions compared to our baseline scenario of around two ppm in two years' time (Figure S6).

Even though the CO_2 change cannot readily be observed, changes in the concentrations of air pollutants can be employed to test the veracity of the bottom-up emission reduction estimates. A decline in NO_2 has been observed globally, and in several countries and cities[7,8]. NO_2 is short-lived (~5 hours), provides

a relatively linear response to emission changes (unlike other pollutants such as O_3 and PM2.5), and reductions in its emissions are expected to be well correlated to CO_2 emission reductions (Figure 2a, Le Quéré et al.). Changes in its concentration thus act as a useful bellwether for changes in CO_2 emissions, however, it remains challenging to get a quantifiable estimate of the emission-driven NO_2 change as it is hard to separate that signal from meteorological variability. To address this we use a machine learning method to derive emission-driven fractional trends from surface air quality monitoring stations around the globe (see methods and Ivatt and Evans, 2019[18]). We aggregate these changes for 32 nations and show how these observationally-based national time-series of NO_2 change compares to our mobility-based estimate of NO_x emissions change in Figure S5. Figure 3 shows the average observationally-derived NO_2 change versus the predicted mobility-based NOx emissions change for each country in 2020. Some differences between the emission estimates and observed changes would be expected: monitoring stations tend to focus on sites with high transport emission and so may be less sensitive to changes in industrial or residential activity; much of the transport emissions of NO_x arises from commercial vehicles (64% of transport emission in the UK[19]) which may show different responses to the population aggregated travel data used here. However, the comparisons for the individual countries (Figure S5) are generally good and there is a quantitative relationship between the average predicted change in the emissions and observed reduction in concentrations (Figure 3). Most countries show a smaller (20% or roughly 2 percentage points) decrease in observed NO_2 than the predicted reduction in NOx emissions, whereas China and India show larger observed reductions than predicted (28% and 48% respectively). This could be due to the Quéré et al. analysis being used to estimate trends in China as Google data was not available and also due a possible lack of representativeness in the phone mobility data for India (see Section 2).

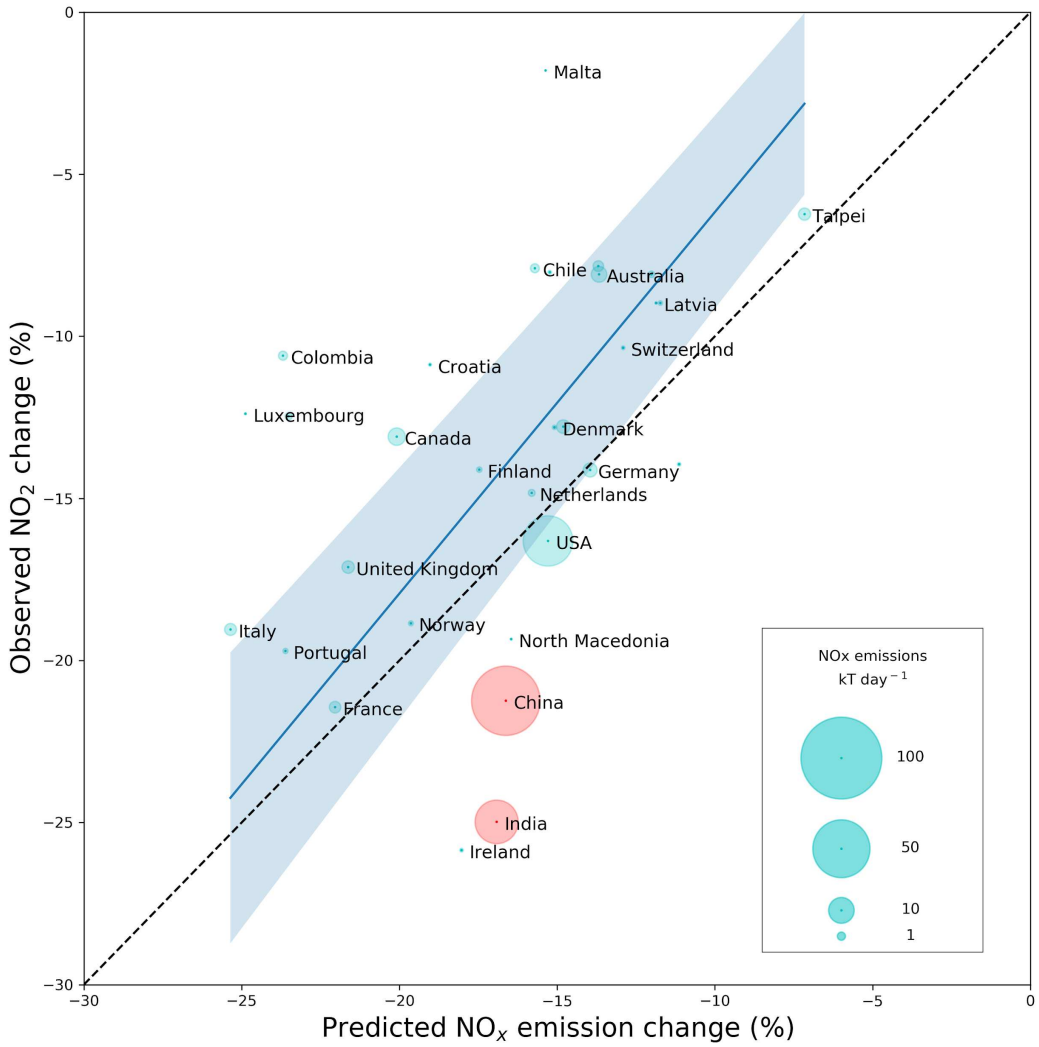

Figure 3. Country level comparison of the observed mean fractional reduction in NO_2 concentration with the mean predicted emissions change in NO_x emissions for the period 1/1/2020 to 11/5/2020. Circle size indicates the mass of NO_x emitted each day for that country from EDGAR emissions. Blue line shows the line of best fit (orthogonal regression) excluding China and India shown in red, weighted by the number of observations in those countries, with the shaded area showing the 95% confidence interval. Not all countries are labelled. Brazil shows an increase in NO_2 concentrations and is not shown but is included in the statistical fit (see Figure S5).

4. Surface temperature response

The immediate response of the warming comes from a combination of an aerosol induced warming trend and a cooling trend both from CO_2 reductions and the NOx-driven tropospheric ozone cooling loss (Figure 4). To estimate the surface temperature response beyond April 2020, the emission trends are projected forward in time under four simple "what-if" assumptions. The temperature changes from these pathways were simulated by the FaIRv1.5 climate emulator[20] which was set up to represent the response expected from the latest generation of climate models (see methods). As we are making a high end estimate of climate change resulting from the pandemic, and as significant social distancing conditions may be necessary for two years[21], we begin by assuming in all three pathways that the emissions decrease will remain at 66% of their April 2020 values until the end of 2021. In the simplest

"two-year blip" pathway emissions return linearly to the baseline pathway by the end of 2022 (Table 1, Figure 5a). This and the other pathways considered are summarised in Table 1.

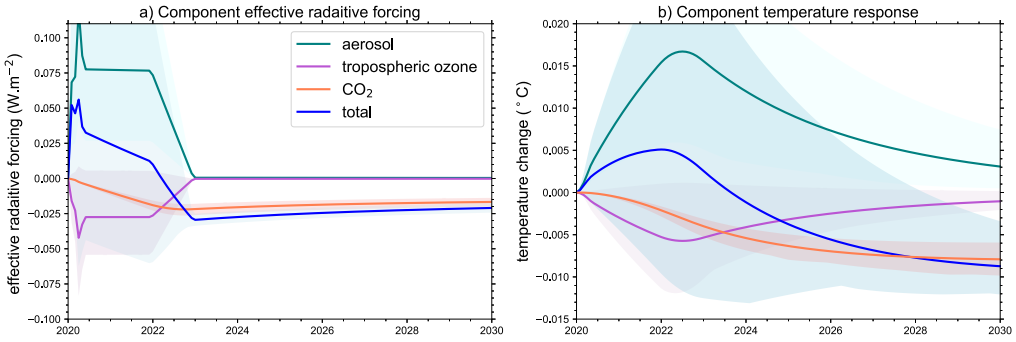

Figure 4. Effective radiative forcing and temperature response for the two-year blip pathway compared to the baseline pathway. The response is broken down by the major forcing contributors, as emulated by the FaIRv1.5 model. 5%–95% Monte-Carlo sampled uncertainties are shown and weighted according to their historical fit to the surface temperature record (see methods).

Table 1, Pathway what-if assumptions

Pathway	What happens	Notes
Baseline	Follows emissions until 2030 consistent with a successful implementation of the current Nationally Determined Contributions (NDC) submitted by individual countries under the Paris Agreement, adapted from Rogelj et al (2017)[15]. Emissions continue after 2030 assuming no significant strengthening in climate action.	The data is adapted from Rogelj et al. (2017)[15] and represents a central estimate of the range of estimates presented therein. This pathway also falls centrally in the range identified by the 2019 UNEP Emissions Gap Report[22]
Two-year blip	Reflecting potential SARS-CoV-2 transmission dynamics[21] this case explores 66% of the April 2020 lockdown persisting until the end of 2021, then emissions linearly recover to baseline by the end of 2022.	This implies a persistent necessity of partial lockdowns until the end of 2023, but with no lasting effect of SARS-CoV-2.
Fossil-fuelled recovery	Follows the two-year blip pathway until end of 2021, then emissions recover in a way similar to the recovery after the 2008/9 global recession, rebounding to 4.5% above where the baseline at the end of 2022. Stimulus packages are designed with strong support for fossil-fuel energy supply, resulting in more fossil investment than a pre-COVID current policy scenario (+1%) and considerably less in low-carbon alternatives (-0.8%). Resulting emissions are 10% higher in 2030 than the baseline scenario, a trend which is assumed to continue thereafter[23].	2030 data taken from Climate Action tracker, "rebound to fossil fuel scenario" with the relative increase in emissions compared to baseline continued thereafter.
Moderate Green stimulus	Follows the two-year blip pathway until end of 2021, then emissions recover slightly, until the end of 2022, but never reach the baseline projections. Governments choose recovery packages to target specifically low-carbon energy supply and energy efficiency, and do not support bailouts for fossil firms. The resulting investment differential (+0.8% for low-carbon technologies and -0.3% for fossil fuels relative to a current-policy scenario), begins to structurally change the intensity of emissions from economic activity, resulting in about a 35% decrease by 2030 relative to the baseline scenario, a trend which is assumed to continue thereafter [23].	Short-term benefits come from changes to the norms of behaviour, then green incentives to decarbonize all sectors of the economy
Strong green stimulus	As the moderate green stimulus with investment differentials (+1.2% for low-carbon technologies and -0.4% for fossil fuels relative to a current policy scenario, resulting in a slightly more than 50% decrease by 2030 relative to the baseline scenario. Also this trend is assumed to continue thereafter.	This has over 50% chance of limiting the 2050 temperature rise to 1.5ºC above preindustrial

Figures 4 and 5 show the effective radiative forcing and temperature response to the "what-if" pathways compared to baseline. Under the two-year blip pathway, due to the cancellation of the influence of short-term pollutants, a longer-term cooling from reductions in CO_2 of around 0.01 ± 0.005 ºC results, compared to the baseline (Figures 4b and S7). Due to the different warming and cooling trends from

short-lived pollutants, the 2020-2030 climate response to the different pathways remains uncertain but is likely negligible whatever path the recovery takes (Figures 4, 5 and S7). However, differences manifest themselves after 2030, where the moderate green stimulus saves around 0.2 ºC of future warming by 2050 and the strong green stimulus saves around 0.3 ºC of future warming (Figure 5).

As the global temperature response due to COVID-19 restrictions will likely be small, climate scientists are encouraged to look for regional climate signatures. In particular changes in aerosol loadings may contribute to increasing regional risks posed by extreme weather such as heat waves or heavy precipitation[24,25]. Such near-term changes require particular attention as hazards posed by extreme weather will compound with the ongoing pandemic situation. As exemplified tragically by tropical cyclone Amphan hitting Kolkata on 21 May 2020. With considerable overlaps of vulnerable groups (for example heat waves and the elderly) or challenges related to the implementation of effective responses (evacuation in case of flooding), as well as potential impacts on crop yields[26] and initial studies suggesting that the spread of COVID-19 may itself be influenced by climatic factors[21], this will put the ability of society and governments to manage compound risks to the test[27].

In our estimates, declines in NOx of greater than 25% that contribute a short-term cooling of up to 0.01 ºC over 2020-2025 almost exclusively from reductions in tropospheric ozone. As the ozone response is expected to have strong regional variation, we test the ozone response in a more sophisticated emulator[28,29] that takes these variations into account (see methods). This estimates an annual mean radiative forcing of -0.029 Wm^{-2} for 2020, in very close agreement with the forcing seen in Figure 4a (-0.030 Wm^{-2}). The emulator also provides an estimate of the regional mean surface ozone changes (Table S5). In contrast to NOx, reductions in emissions of other short-lived pollutants, especially SO_2, cause a warming from a weakening negative aerosol forcing. These two effects more or less cancel in our simulations, although on balance we expect a small warming effect over the next 5 years (Figure 4).

In spite of the uncertainty, our results indicate that reductions of NOx have a cooling effect which will likely offset a considerable fraction of the warming that comes from reductions in emissions of other short-lived pollutants. This suggests that policies directed at limiting pollution from road transport could offset the short-term warming that might come from policies that reduce pollution from the power and industry sector. Therefore, we recommend policies are enacted to cut pollution from all three sectors at the same time. This is a useful way forward for net-zero transition pathways so we can avoid any short-term warming effects that might come from reductions in aerosol pollution[30].

Figure 5 shows estimated changes in CO_2 emissions and the climatic responses for the four assessed pathways. We find that both the two-year blip pathway, where the economic recovery maintains current investment levels, or the fossil fuelled recovery pathway, are likely to exceed a 2ºC above preindustrial limit by 2050 (>80%, Figure S8). Conversely, choosing a pathway with strong green stimulus assumptions (~1.2% of global GDP), including climate policy measures, has a good chance (~55%, Figure S8) to keep global temperatures change above preindustrial within the 1.5ºC limit.

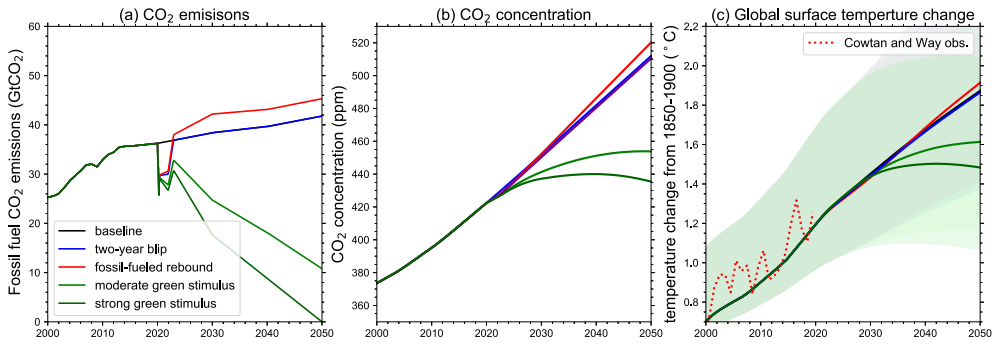

Figure 5. a) Emissions of CO_2, b) CO_2 concentrations, c) the surface air temperature response for the what-if pathways from Table 1, emulated by the FaIRv1.5 model. The baseline pathway is also plotted, but largely obscured by the two-year-blip pathway. 5%–95% Monte-Carlo sampled uncertainties are shown and weighted according to their historical fit to observations[31] shown in panel c (see methods).

Our work has shown that the global temperature signal due to the short-term dynamics of the pandemic are likely to be small, highlighting that even with massive shifts in behaviour, without underlying system-wide decarbonisation of economies any reduction in the rate of warming would be modest. However, we can change the expected 2050 warming level, depending economic investment choices and there is the potential for keeping the Long-Term Temperature Goal of the Paris Agreement within sight.

Lastly, by combining large datasets from surface air quality networks with mobility data, we have illustrated the science benefits from timely and easy access to big data. Such data syntheses can help epidemiology and environmental sciences provide the evidence base for the solutions that are urgently needed to build a resilient recovery to the devastating pandemic. Google, Apple and other big data providers are encouraged to continue to provide and expand their data offerings.

Methods

a) CO_2 emission estimates

The Google Mobility analysis.

Google[4] and Apple[5] mobility data were accessed on 21 May 2020. National average Google data was used for 114 countries, and the US states. Mobility was provided in 6 categories of which we used four in our analyses (transit stations, residential, work places, retail and recreation) Apple mobility data was from phone movement changes available for 63 countries providing data on changes in transit use, walking and driving, depending on country. Google data was based on assigned phone locations and was referenced to the day of the week average in the 5-week period Jan 3–Feb 6, 2020. Apple employed a baseline of 13 February and did not account for day of week effects. The Apple data was considerably more variable and was only used as a check on the other datasets. Our tests found that the Google transit trends agreed well with Apple driving trends in the 60 nations with overlapping data (Figures 1a and S1) and this gave us confidence to employ the Google transit trends as an estimate of general trends in emissions from land-based surface transport. As discussed in the main text, we expect the Google mobility data to overestimate emission trends in the other sectors and we compare our new approach for estimating granular near real time emission changes with the previous approach of Le Quéré et al.[2] and with observations to test the approach.

The Le Quéré et al. sector analysis.
Le Quéré et al. analysed emission changes in eight sectors (power, surface transport, residential, public and commercial, industry, national shipping, international shipping, national aviation and international aviation), and 69 countries representing 97% of global emissions. The Le Quéré et al. estimates are based on a global estimate of sector emission reductions according to a 1-3 level of confinement. Changes in emissions were estimated by quantifying changes in individual and industrial activity, in each sector as a function of the level of confinement in respective countries. The data is then extrapolated for each country and each day depending on their level of confinement and their mean emissions in each sector. The USA and China were treated at the state and provincial level, respectively. Projections for 2020 were also provided. Low, medium, and high estimates of the emission changes resulting from different confinement levels were tested against our data. It was found that the high estimates agreed best with the Google transit trends over January-May 2020 (see Figures 1, S1 and 2b).

Mobility-based emission estimates.
As mobility analysis does not cover all sectors or countries to make a global emission estimate we combine the mobility analysis with components of the analysis in Le Quéré et al. to estimate global emission changes for CO_2 and other pollutants that were due to the COVID-19 restrictions.

We adopt the sector approach of Le Quéré et al., but substitute their percentage changes in the emissions from surface transport, residential, public and commercial and industry sectors, with Google mobility changes in transit, residential, retail and recreation, and workplaces respectively. For the power sector, we employed a hybrid approach, using a combined weighting of workplace, residential and retail mobility weighted by the 2019 national split of industrial, residential and commercial emissions. Then we used this weighted mobility measure to scale the power sector emissions. Finally applying a scaling to match the global emission change in the power sector of the Le Quéré et al. high end estimate. We also directly employed the Le Quéré et al. emission trends for international and national aviation and shipping. In the 45 countries with only Google data available, the average emission changes from the 69 Le Quéré et al. nations were employed in the sectors not covered by the Google mobility data. Note that for simplicity and following Le Quéré et al., shipping changes are added to the surface transport trends in the analyses presented in Figure 2 and Figure S3. All emission changes are compared to a daily emission rate which is the annual averaged 2019 emission estimated for that country divided by 365 (using the data and approach from Le Quéré et al.). The combined dataset gives daily CO_2 emission changes for 2020, across 8 sectors and 123 countries, covering 99% of global emissions. The Le Quéré et al. high-end estimate and new mobility-based emission estimates were found to agree well with each other, both at the individual US state level and at the country level for the 56 countries with overlapping data (Figures S1, S2 and Figure 1b).

Table S2 compares the global average trends and that from some major nations to the CO_2 estimates in Le Quéré et al. and that of Liu et al.[1]. Our trends are expected to be higher than the other datasets, but this doesn't manifest itself for first quarter trends in all countries. As the Google trends only start on 15 February, our analysis will underestimate first quarter trend estimates where changes occurred before this date. Our change estimates agree well with Le Quéré et al. high-end estimate for March and April (see Table S3). More interesting are the differences with the Liu et al. dataset for India and Russia, where their trends are considerably smaller. This could be caused by the differences with the reference assumptions. The Liu et al. approach makes a daily reference comparison with 2019 emissions and both nations show declining emissions in the first quarter of 2019, whereas our reference is taken as the Google mobility base-period of 3 January to 3 February (see methods). As the Le Quéré et al. confinement levels are well correlated in time with the Google mobility estimates and also

quantitatively agree (see Figure S2), we assume that the mobility trends we see are largely a response to COVID 19. However, more work will be needed to fully understand and resolve these differences.

a) Non-CO_2 emission estimates

The Emission Database for Global Atmospheric Research (EDGAR) version 5.0 database[14] provides gridded and national level sectorial emissions on methane, nitrous oxide and several short-lived species. The last year available is 2015. The sectors employed in the EDGAR analyses are mapped onto the Le Quéré et al. sectors used here, according to the breakdown in Table 2. The national and sector level emission changes for 2020 are then estimated by equation 1.

$$\Delta \boldsymbol{E_{in,is}(t)} = \boldsymbol{Ebase_{in,is}} \frac{\Delta \boldsymbol{C_{in,is}(t)}}{\boldsymbol{Cbase_{in,is}}} \quad (\mathbf{1})$$

Where $\Delta \boldsymbol{E_{in,is}(t)}$ is the emission change (in ktday^{-1}) of the species as a function of nation ($\boldsymbol{in}$) and sector ($\boldsymbol{is}$). $\boldsymbol{Ebase_{in,is}}$ is the annual emission divided by 365 of the species from the sector and nation for 2015, see Table S1. $\Delta \boldsymbol{C_{in,is}(t)}$ and $\boldsymbol{Cbase_{in,is}}$ are the CO_2 emission change over 2020, and the average daily baseline emission respectively in the sector and nation being considered (CO_2 is in units of $MtCO_2$ day^{-1}). Similar equations are used for international aviation and shipping, where the global emission from aviation or shipping is ratioed by the globally averaged CO_2 emission change in the corresponding sum over the national change in sectors from the Le Quéré et al. data. The resulting changes are shown in Figures 2,3, S3 and S4. Note that although nearly all global CO_2 emissions were accounted for in Le Quéré et al., agricultural and waste emissions are excluded in the non-CO_2 analyses as they are assumed not to change. This leads to a reduced fraction of global emissions for non-CO_2 gases being covered and smaller emission changes for many species (Figure 3).

Table 2. EDGAR sector matching to Le Quéré et al. sectors.

Species	Le Quéré et al. (2020) sector categories						
	Surface transport	Residential	Public/Commercial	Industrial	Power	Shipping	Aviation
SO_2, NOx, NMVOCs, OC, BC, CO,NH_3	'Road Transportation no resuspension', 'Road Transportation resuspension', 'Rail transportation','Other transportation'	Other Sectors	None	'Manufacturing Industries and Construction', 'Chemical Industry', 'Metal Industry', 'Cement production', 'Lime production', 'Glass Production', ' Other Process Uses of Carbonates'	'Main Activity Electricity and Heat Production', 'Solid Fuels', 'Petroleum Refining - Manufacture of Solid Fuels and Other Energy Industries', 'Oil and Natural Gas'	'Water-borne Navigation', 'International Shipping'	'Civil Aviation', 'International Aviation'
CH_4, N_2O	'Road Transportation', 'Railways', 'Other Transportation'	Other Sectors	None	'Manufacturing Industries and Construction', 'Chemical Industry', 'Metal Industry'	'Main Activity Electricity and Heat Production', 'Solid Fuels', 'Petroleum Refining - Manufacture of Solid Fuels and Other Energy Industries', 'Oil and Natural Gas'	'Water-borne Navigation', 'International Shipping'	'Civil Aviation', 'International Aviation'

b) Emission scenarios

The generated datasets above firstly combine sector specific mobility changes referenced to the 3 January to 6 February 2020 period, with national lockdown measures. The method then uses published national emission inventories for either 2019 (for CO_2) or 2015 (for non-CO_2) to derive absolute emission changes which would also be relative to the early 2020 period. This reference is then projected

out to 2030 to form a emission baseline representing current Nationally Determined Contributions (NDCs)[15]. To explore the temperature response to emission changes relative to this baseline, the bottom-up emission change estimates from the first four months of 2020 have been extended according to the scenarios illustrated in Table 1. Four scenarios are explored: "two-year blip", "fossil-fuelled recovery", "moderate green stimulus", and "strong green stimulus". The "two-year blip" scenario assumes climate action to continue at the same level of ambition as implied by the current NDCs[15] until 2030 – approximated by the implied global carbon price consistent with the emission reduction resulting from the NDCs. The "fossil-fuelled recovery" follows a path that lies 10% higher than the NDC path. The "moderate green stimulus" assumes about a 35% reduction in total global greenhouse gas emissions relative to the baseline NDC path and a further decline of global CO_2 emissions towards zero emissions in 2060. Non-CO_2 emissions after 2030 are completed in proportions consistent with the MESSAGE-GLOBIOM implementation of the middle-of-the-road Shared Socioeconomic Pathway (SSP2)[32,33]. The "strong green stimulus" assumes about a 52% reduction in total global greenhouse gas emissions relative to the baseline NDC path and a further decline of global CO_2 emissions towards zero emissions in 2050. Non-CO_2 emissions are completed in proportions consistent with the sustainability Shared Socioeconomic Pathway (SSP1) implemented by the IMAGE model[34]. Scenarios are given as emissions of 39 species from anthropogenic and natural sources and volcanic and solar radiative forcing (see Smith et al.[20] for details). Only the ten species evaluated in this paper are changed. The original dataset gives annual emissions from 1750-2100, and these are linearly interpolated to monthly values, to provide higher time resolution for the subsequent calculations of effective radiative forcing and temperature.

c) Comparison to NO_2 observations

Hourly observations of NO_2 are taken from the OpenAQ database (https://openaq.org/) between January 1, 2018 and May 3, 2020, giving 1,747,189 hourly observations from 2,873 sites around the world. For each observation, a spatially and temporally co-located model value for the meteorological, chemical and emissions state is acquired from the NASA GEOS Composition Forecast (GEOS-CF) system. GEOS-CF integrates the GEOS-Chem chemistry model into the GEOS Earth System Model[35] providing global hourly analyses of atmospheric composition at 25x25 km^2 spatial resolution in near real-time. Anthropogenic NO_x emissions are prescribed using monthly HTAP bottom-up emissions[36], with annual scale factors based on OMI satellite data applied to it to account for year-over-year changes. GEOS-CF does not account for emission reductions related to COVID-19, providing a business-as-usual estimate of NO_2 that serves as a reference baseline for surface observations. For each site, a function describing the time dependent model bias (observed value - modelled value) is developed using the 2018 and 2019 observations based on the XGBoost algorithm[37], with the model meteorological, chemical and emissions state as the dependent variables. 50% of this data is used for training, and 50% used for testing. For 2020, we predict the concentration of NO_2, by taking the model output time series of NO_2 at each station and add the bias predicted by our trained algorithm. This then provides a counterfactual for the NO_2 concentration had COVID-19 restrictions not been put into place. We calculate the ratio between the actual concentration and that predicted for each site and then take the mean across all sites within a country. These data are compared to 26 country level emission estimates in Figure S5, and the country-mean reductions compared to that predicted from the mobility data is shown in Figure 2b.

d) Surface temperature change estimates

From the emission scenarios in Section 3, global averaged effective radiative forcing (ERF) and near-surface air temperature are computed. First, ERFs are calculated using the FaIR version 1.5 model and

the methodology outlined in Smith et al. (2018)[20] for 13 different forcing components. Uncertainties are estimated by 10,000 Monte Carlo samples of relative ERF uncertainties, using ranges based on IPCC AR5[38], see Smith et al. (2018) for details. NOx emissions affect direct forcing from nitrate aerosol and tropospheric ozone radiative forcing. Additionally, the ERF from aviation contrails and contrail-induced cirrus is assumed to scale with NOx emissions from the aviation sector.

The two layer energy balance model of Geoffroy et al.[39,40] including efficacy of deep ocean heat uptake is used to translate these ERF time series into surface temperature estimates. The five free parameters in this model are chosen to match individual Climate Model Intercomparison Project phase 6 (CMIP6) model behaviour by fitting the parameters to $4xCO_2$ abrupt simulations in 35 models; these parameter fits are shown in Table S4. To estimate uncertainties, parameters corresponding to an individual model are picked randomly 10,000 times and paired to a sampled ERF parameter range for each of the 13 ERF timeseries. The two-layer model is then run with each of these parameter sets to make a surface temperature projection. The resulting plume of possible projections is then compared to Cowtan and Way[31] observed surface temperature record. The Cowtan and Way data has been adjusted to allow for the fact the near-surface air temperature has warmed more than the sea surface temperature. To make this adjustment, the CMIP6 ratio of near-surface air temperature to blended near surface air temperature and surface ocean temperatures is made over the historical period and found to converge towards 8% in recent years[41]. This is then used to scale the observations upwards. The root mean square error of the simple model projections are then compared to these scaled observations over 1850-2019 inclusive. The goodness of fit is then used to provide projected probability distribution based on a weighted average of the goodness of fit. This follows the method outlined in Knutti et al.[42], with the exception that we do not downweight ensemble members based on independence.

e) Testing the ozone forcing parameterisation

The FaIRv1.5 model used above adopts a simple global annual mean emission-forcing relationship for tropospheric ozone which may not capture the seasonal and regional nuances of the atmospheric chemical response to the changes in NOx and other emissions. To test this a second ozone parameterisation was employed based upon source-receptor relationships from models that participated in the Task Force on Hemispheric Transport of Air Pollutants (TF-HTAP) project[43]. The parameterisation[28,29] emulates the ozone response in models to applied perturbations in ozone precursor emissions (NOx, CO and NMVOCs) and global CH_4 abundance. For emission perturbations in CO and NMVOCs a linear scaling factor is used whereas a non-linear factor is used for changes in NOx and CH_4. The 2020 annual mean tropospheric ozone radiative forcing and annual mean tropospheric ozone burden change deduced from this parameterisation were -0.029 Wm^{-2} and 7.5 Tg for the high emission scenario used here.

References

1. Liu, Z. *et al.* COVID-19 causes record decline in global CO2 emissions. *http://arxiv.org/abs/2004.13614* (2020).
2. Le Quéré, C. *et al.* Temporary reduction in daily global CO2 emissions during the COVID-19 forced confinement. *Nat. Clim. Chang.* 1–7 (2020). doi:10.1038/s41558-020-0797-x
3. COVID-19 Worldwide Air Quality data. Available at: https://aqicn.org/data-platform/covid19/. (Accessed: 24th May 2020)
4. Google LLC Community Mobility Reports. Available at: https://www.google.com/covid19/mobility/. (Accessed: 24th May 2020)
5. Apple LLC Mobility Trends Reports. Available at: https://www.apple.com/covid19/mobility. (Accessed: 24th May 2020)
6. COVID-19 Map - Johns Hopkins Coronavirus Resource Center. Available at: https://coronavirus.jhu.edu/map.html. (Accessed: 24th May 2020)

7. Bauwens, M. *et al.* Impact of coronavirus outbreak on NO 2 pollution assessed using TROPOMI and OMI observations. *Geophys. Res. Lett.* (2020). doi:10.1029/2020GL087978
8. Shi, X. & Brasseur, G. P. The Response in Air Quality to the Reduction of Chinese Economic Activities during the COVID-19 Outbreak. *Geophys. Res. Lett.* **submitted**, (2020).
9. China's air pollution overshoots pre-crisis levels for the first time. Available at: https://energyandcleanair.org/china-air-pollution-rebound-briefing/. (Accessed: 24th May 2020)
10. Zhang, R. *et al.* NOx Emission Reduction and Recovery during COVID-19 in East China. *Atmosphere (Basel).* **11**, 433 (2020).
11. Friedlingstein, P. *et al.* Global carbon budget 2019. *Earth Syst. Sci. Data* **11**, 1783–1838 (2019).
12. Domestic energy usage patterns during social distancing | Octopus Energy. Available at: https://octopus.energy/blog/domestic-energy-usage-patterns-during-social-distancing/. (Accessed: 24th May 2020)
13. Operating System Market Share Worldwide | StatCounter Global Stats. Available at: https://gs.statcounter.com/os-market-share#quarterly-201903-201903-map. (Accessed: 24th May 2020)
14. Crippa, M. *et al.* High resolution temporal profiles in the Emissions Database for Global Atmospheric Research. *Sci. Data* **7**, 1–17 (2020).
15. Rogelj, J. *et al.* Understanding the origin of Paris Agreement emission uncertainties. *Nat. Commun.* **8**, 1–12 (2017).
16. Joos, F. *et al.* Carbon dioxide and climate impulse response functions for the computation of greenhouse gas metrics: a multi-model analysis. *Atmos. Chem. Phys.* **13**, 2793–2825 (2013).
17. Jones, C. D. *et al.* Simulating the Earth system response to negative emissions. *Environ. Res. Lett.* **11**, 95012 (2016).
18. Ivatt, P. & Evans, M. Improving the prediction of an atmospheric chemistry transport model using gradient boosted regression trees. *Atmos. Chem. Phys. Discuss.* 1–33 (2019). doi:10.5194/acp-2019-753
19. Richmond B & Misra A. *UK Informative Inventory Report (1990 to 2018)*. (2020).
20. Smith, C. J. *et al.* FAIR v1.3: A simple emissions-based impulse response and carbon cycle model. *Geosci. Model Dev.* **11**, (2018).
21. Kissler, S. M., Tedijanto, C., Goldstein, E., Grad, Y. H. & Lipsitch, M. Projecting the transmission dynamics of SARS-CoV-2 through the postpandemic period. *Science (80-.).* **368**, eabb5793 (2020).
22. Emissions Gap Report 2019 | UNEP - UN Environment Programme. Available at: https://www.unenvironment.org/resources/emissions-gap-report-2019. (Accessed: 24th May 2020)
23. Action Tracker, C. *Climate Action Tracker UPDATE A government roadmap for addressing the climate and post COVID-19 economic crises Summary and conclusions*.
24. Luo, F. *et al.* Projected near-term changes of temperature extremes in Europe and China under different aerosol emissions. *Environ. Res. Lett.* **15**, 034013 (2020).
25. Samset, B. H. *et al.* Climate Impacts From a Removal of Anthropogenic Aerosol Emissions. *Geophys. Res. Lett.* (2018). doi:10.1002/2017GL076079
26. Dentener, F. *et al.* Lower air pollution during COVID-19 lock-down: improving models and methods estimating ozone impacts on crops. doi:10.31223/OSF.IO/DE9FS
27. Phillips, C. A. *et al.* Compound climate risks in the COVID-19 pandemic. *Nat. Clim. Chang.* 1–3 (2020). doi:10.1038/s41558-020-0804-2
28. Turnock, S. T. *et al.* The impact of future emission policies on tropospheric ozone using a parameterised approach. *Atmos. Chem. Phys.* **18**, 8953–8978 (2018).
29. Turnock, S. T., Wild, O., Sellar, A. & O'Connor, F. M. 300 years of tropospheric ozone changes using CMIP6 scenarios with a parameterised approach. *Atmos. Environ.* **213**, 686–698 (2019).
30. Shindell, D. & Smith, C. J. Climate and air-quality benefits of a realistic phase-out of fossil fuels. *Nature* **573**, 408–411 (2019).
31. Cowtan, K. & Way, R. G. Coverage bias in the HadCRUT4 temperature series and its impact on recent temperature trends. *Q. J. R. Meteorol. Soc.* **140**, 1935–1944 (2014).
32. Rogelj, J. *et al.* Scenarios towards limiting global mean temperature increase below 1.5 °C. *Nat. Clim. Chang.* **8**, 325–332 (2018).
33. Fricko, O. *et al.* The marker quantification of the Shared Socioeconomic Pathway 2: A middle-of-the-road scenario for the 21st century. *Glob. Environ. Chang.* **42**, 251–267 (2017).
34. van Vuuren, D. P. *et al.* Energy, land-use and greenhouse gas emissions trajectories under a green growth paradigm. *Glob. Environ. Chang.* **42**, 237–250 (2017).
35. Hu, L. *et al.* Global simulation of tropospheric chemistry at 12.5 km resolution: performance and evaluation of the GEOS-Chem chemical module (v10-1) within the NASA GEOS Earth system model (GEOS-5 ESM). *Geosci. Model Dev.* **11**, 4603–4620 (2018).
36. Janssens-Maenhout, G. *et al.* HTAP_v2.2: a mosaic of regional and global emission grid maps for 2008 and 2010 to study hemispheric transport of air pollution. *Atmos. Chem. Phys.* **15**, 11411–11432 (2015).

37. Chen, T. & Guestrin, C. XGBoost: A scalable tree boosting system. in *Proceedings of the ACM SIGKDD International Conference on Knowledge Discovery and Data Mining* **13-17-August-2016**, 785–794 (Association for Computing Machinery, 2016).
38. Myhre, G. *et al.* Anthropogenic and Natural Radiative Forcing. in *Climate Change 2013 - The Physical Science Basis* (ed. Intergovernmental Panel on Climate Change) 659–740 (Cambridge University Press, 2013). doi:10.1017/CBO9781107415324.018
39. Geoffroy, O. *et al.* Transient Climate Response in a Two-Layer Energy-Balance Model. Part I: Analytical Solution and Parameter Calibration Using CMIP5 AOGCM Experiments. *J. Clim.* **26**, 1841–1857 (2013).
40. Geoffroy, O. *et al.* Transient Climate Response in a Two-Layer Energy-Balance Model. Part II: Representation of the Efficacy of Deep-Ocean Heat Uptake and Validation for CMIP5 AOGCMs. *J. Clim.* **26**, 1859–1876 (2013).
41. Richardson, M., Cowtan, K., Hawkins, E. & Stolpe, M. B. Reconciled climate response estimates from climate models and the energy budget of Earth. *Nat. Clim. Chang.* **6**, 931–935 (2016).
42. Knutti, R. *et al.* A climate model projection weighting scheme accounting for performance and interdependence. *Geophys. Res. Lett.* **44**, 1909–1918 (2017).
43. Koffi, B. *et al. Hemispheric Transport of Air Pollution (HTAP) specification of the HTAP2 experiments : ensuring harmonized modelling.* (2016). doi:10.2788/725244

Acknowledgements
Funding was provided by the European Union's Horizon 2020 Research and Innovation Programme under grant agreement nos. 820829 (CONSTRAIN) and UKRI NERC grant NE/N006038/1 (SMURPHS). CDJ was supported by the Joint UK BEIS/Defra Met Office Hadley Centre Climate Programme (GA01101) and CRESCENDO (EU Project 641816). CLQ was supported by the Royal Society (grant no. RP\R1\191063), and the European Commission H2020 4C grant (no. 821003). MJE is grateful for computational support from the University of York's HPC service (Viking). Stella Forster is thanked for proofreading the paper and for useful ideas.

Data Availability
A GitHub repository of the generated datasets and is available from https://github.com/Priestley-Centre/COVID19_emissions
Google LLC mobility data is available from https://www.google.com/covid19/mobility/
Apple LLC mobility data is available from https://www.apple.com/covid19/mobility
EDGAR gridded emissions data is available from https://data.europa.eu/doi/10.2904/JRC_DATASET_EDGAR
Cowtan & Way temperature observations are available from https://www-users.york.ac.uk/~kdc3/papers/coverage2013/had4_krig_annual_v2_0_0.txt
Le Quéré et al. (2020) emissions data are available from https://www.icos-cp.eu/gcp-covid19
The air quality data is available from https://openaq.org/. The GEOS modelled air pollution data used in this study/project have been provided by the Global Modeling and Assimilation Office (GMAO) at NASA Goddard Space Flight Center and is available from https://opendap.nccs.nasa.gov/dods/gmao/geos-cf/assim .

Author roles
PMF and HIF designed the study and PMF performed the main analyses with contributions from HIF. CLQ provided the original data and contributed design ideas. CJS provided the CMIP6 tuning of the two layer model. CK and ME provided the surface NO_2 analyses. ST provided the ozone emulator analyses. MG, C-FS contributed future scenario ideas. JR provided the scenario emission data with contributions from RL. CDJ contributed the CO_2 concentration change discussion. DR contributed the wider air quality and societal context discussion. TR provided the gridded online materials. All authors contributed to the writing.

Supplementary Information

Figure S1. Decrease in mobility for April 2020, computed from the average of Google[4], Le Quéré et al.[2] and Apple data[5], depending on which of the three datasets are available in the specified country. The average is shown as the grey bars. The available Google mobility data trends from transit stations, Apple driving data trends and the Le Quéré et al. high-end estimate for surface transport emission changes are shown as the coloured symbols, from which the average is derived.

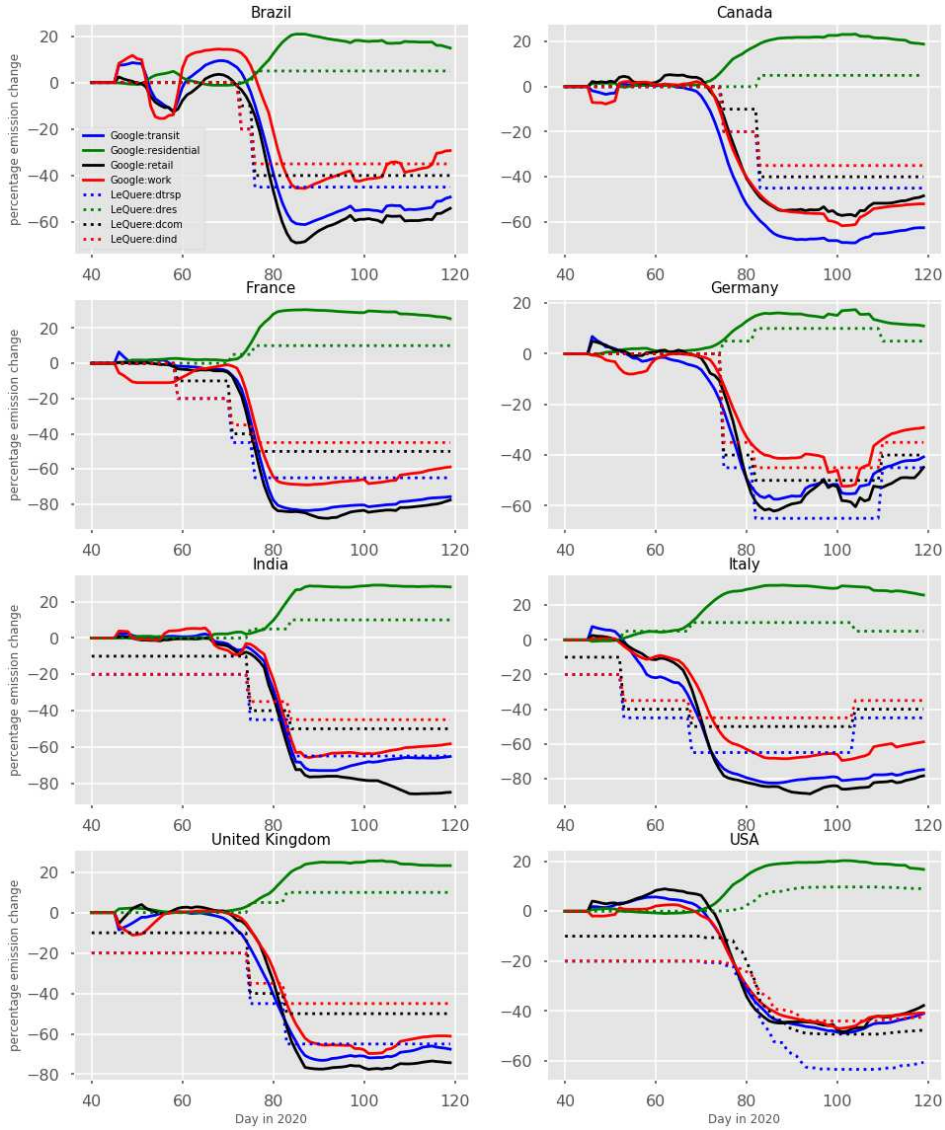

Figure S2: National sector specific emission trends for example nations. Data from Google (solid lines) and Le Quéré et al. (dotted lines) using the high end of the uncertainty range. Sectors shown from Le Quéré et al are transport (blue), residential (green), public and commercial (black) and Industry red. Corresponding Google trends are shown in transit mobility (blue), residential (green), retail (black) and workplaces (blue). A 7-day running mean is applied to the Google data.

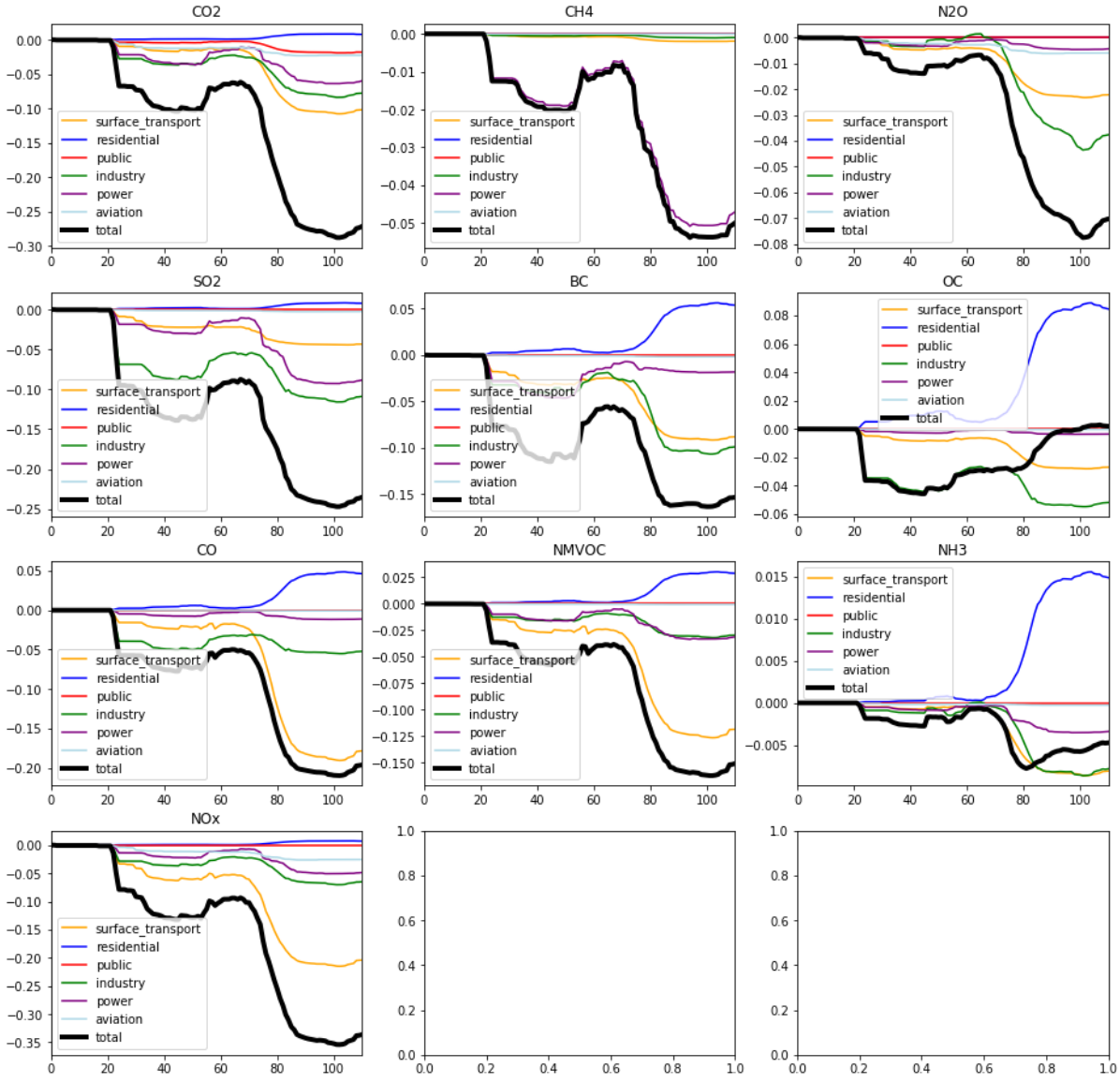

Figure S3. Global average absolute emission change in a given sector for the high scenario by pollutant as a fraction of the daily average emission for that gas summed across all sectors. Following Le Quéré et al., shipping changes are added to the surface transport trends.

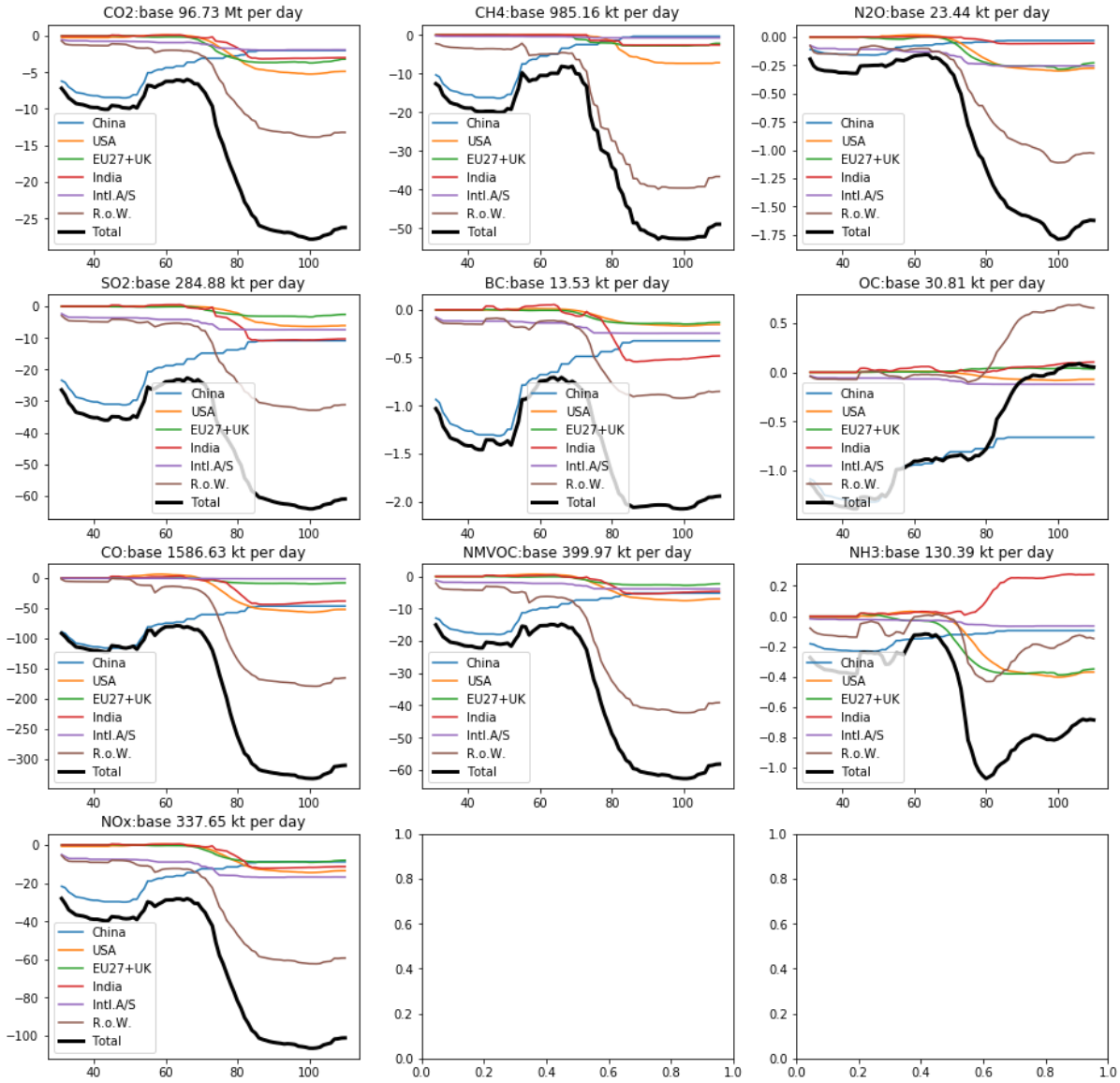

Figure S4. Global averaged emission change by pollutant in kt per day (Mt per day for CO_2). The annually averaged daily emission is shown in the title. Major emitting nations and regions, as well as aviation are shown.

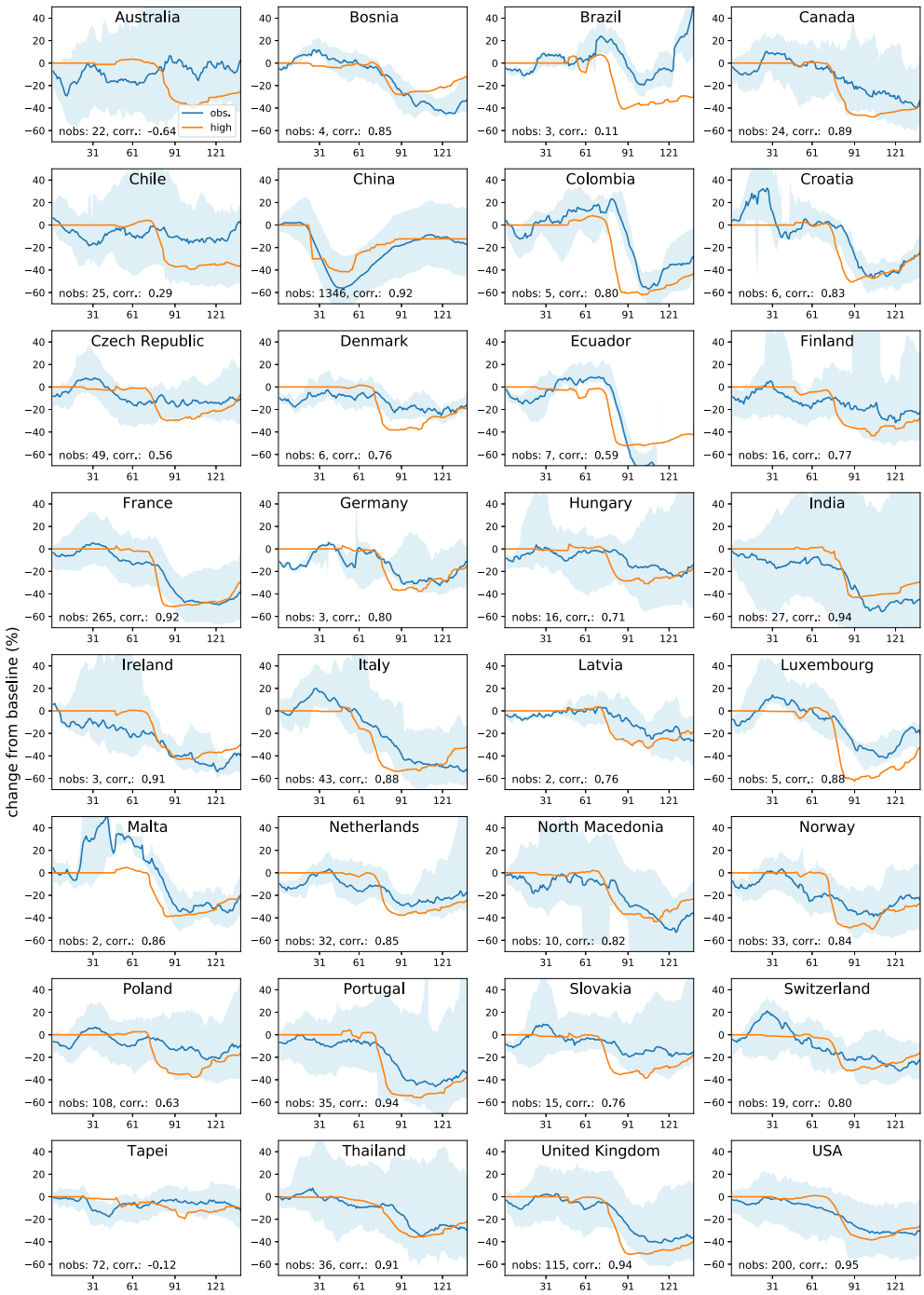

Figure S5. Time series of predicted fractional changes in NO_x emission for 2020 from our emission estimate, with the median fractional change in observed surface NO_2 concentrations compared to a non-COVID counterfactual for 32 nations (see methods). Where more than one surface station is available the 5% and 95% uncertainty ranges in the observations are shown. The number of national surface stations employed for analysis and the correlation coefficient between the two estimates is given in each panel.

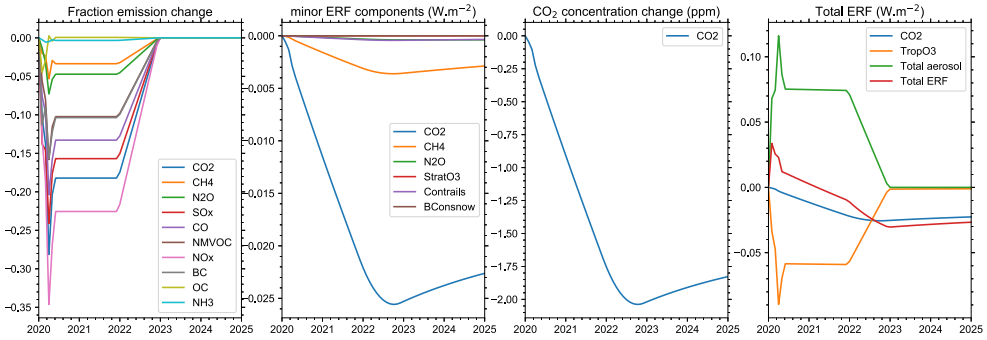

Figure S6. Emissions, and best estimates of CO_2 concentration and effective radiative forcing (ERFs) components from the two-year blip scenario. Component ERFs are shown with minor ERFs in panel b) and the three largest ERF changes in c).

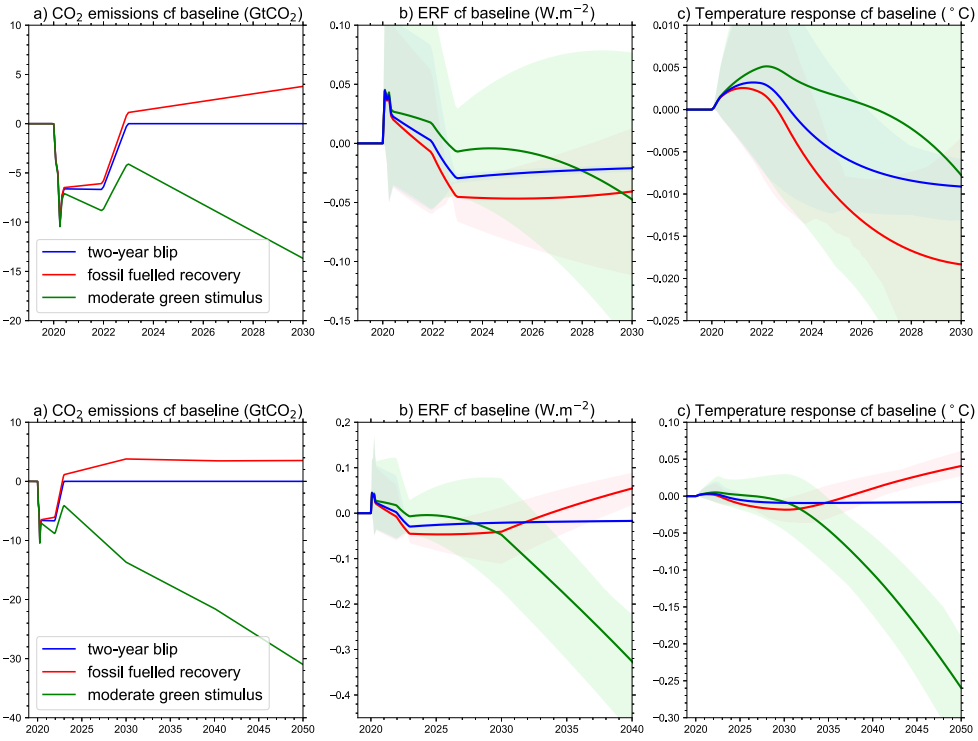

Figure S7. Emissions, ERF and temperature response from the three scenarios over 2019-2030 (top) and 2019 to 2050 (bottom) . The probabilities are generated by varying the emulated CMIP6 model (one of 35) and ERF ranges with a 10,000 Monte Carlo sample. Distributions are weighted according to their goodness of fit over the historical period (see methods).

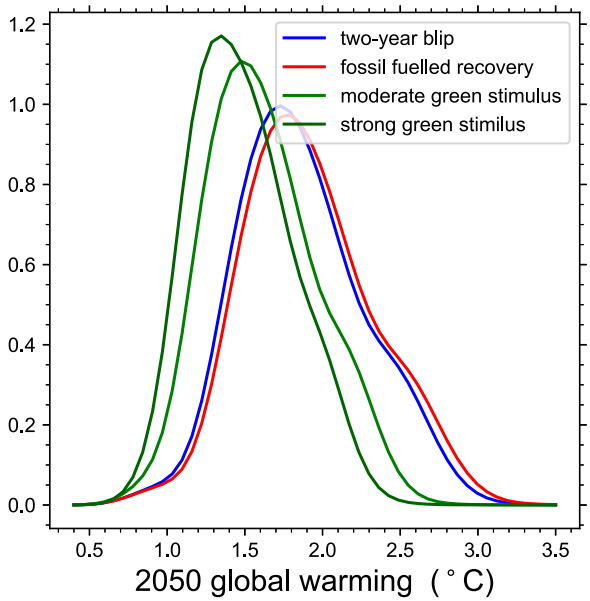

Figure S8. Probability distributions of 2050 global warming levels above 1850-1900 for the scenarios in Table 1, generated by varying the emulated CMIP6 model (choosing one of 35 model formulations) and ERF ranges. Distributions are weighted according to their goodness of fit over the historical period (see methods).

Table S1 Percentage emission change in emitted species for the first four months of 2020 and an estimate of the annual change if lockdown continues at 66% of the April level.

CO2		January	February	March	April
	Global	-1.7	-9.2	-14.6	-27.5
	China	-6.1	-29.4	-12.4	-7.9
	India	-0.1	0	-15.1	-41.7
	USA	-0.1	-1.1	-12.9	-35.2
	EU27+UK	-0.1	-1.1	-12.9	-35.2
	Russia	0	-6.8	-14.9	-31.8
	Japan	-0.1	-1.2	-6	-25
	Brazil	0	-0.4	-14.1	-39.4
CH4		January	February	March	April
	Global	-0.3	-1.7	-2.5	-5
	China	-1.5	-7.9	-1.5	-0.2
	India	0	0	-1.1	-2.9
	USA	0	0	-2.3	-10.2
	EU27+UK	0	0	-2.3	-10.2
	Russia	0	0	-5	-16
	Japan	0	0	-0.3	-1.9
	Brazil	0	0	-0.6	-1.2
N2O		January	February	March	April
	Global	-0.2	-1.1	-3.2	-7
	China	-0.7	-3.7	-1.4	-0.8
	India	0	0	-1.1	-3.1
	USA	0	0	-3.9	-10.5
	EU27+UK	0	0	-3.9	-10.5
	Russia	0	-5.8	-8.9	-14.9
	Japan	0	-0.7	-3.6	-11.7
	Brazil	0	0	-0.5	-1.5
SO2		January	February	March	April
	Global	-2.2	-11.4	-13.4	-21.6
	China	-6.9	-32.8	-17.6	-12.9
	India	0	0.2	-12.2	-33.4
	USA	0	-0.3	-7.1	-26
	EU27+UK	0	-0.3	-7.1	-26
	Russia	0	-4.5	-11.7	-27.1
	Japan	0	-1.1	-5.7	-23.1
	Brazil	0	-0.4	-7.3	-24.2
BC		January	February	March	April
	Global	-1.8	-9.4	-9.3	-14.7
	China	-6.4	-31.7	-13.7	-9
	India	0	0.4	-8	-23
	USA	0	0.1	-10.4	-29
	EU27+UK	0	0.1	-10.4	-29
	Russia	0	-7.6	-13.6	-26.2
	Japan	0	-1.5	-9.4	-34.7
	Brazil	0	-0.3	-7.4	-23.4
OC		January	February	March	April
	Global	-0.9	-4	-2.4	0.1
	China	-3.8	-16.9	-11.3	-9.3
	India	0	0.3	0.5	1.7
	USA	0	0.1	-2.6	-7.8
	EU27+UK	0	0.1	-2.6	-7.8
	Russia	0	-2.8	-3.9	-5.7
	Japan	0	-1.6	-9.8	-26.4
	Brazil	0	0	-1.1	-4.3
CO		January	February	March	April
	Global	-1.4	-6.9	-11.1	-20
	China	-6.3	-29.5	-17.1	-13.1
	India	0	0.3	-7	-19.9
	USA	0	1.1	-14	-38.1
	EU27+UK	0	1.1	-14	-38.1
	Russia	0	-10.9	-19.8	-38.6
	Japan	0	-2	-10.9	-29.5
	Brazil	0	-0.1	-6.9	-19.5
NMVOC		January	February	March	April
	Global	-0.9	-4.9	-8.3	-14.9
	China	-3.8	-18.6	-8.8	-6.2
	India	0	0.3	-4.8	-13.3
	USA	0	0.6	-8	-23.5
	EU27+UK	0	0.6	-8	-23.5
	Russia	0	-8	-16.1	-33.7
	Japan	0	-0.8	-5	-14.5
	Brazil	0	-0.2	-8	-23
NH3		January	February	March	April
	Global	0	-0.2	-0.4	-0.5
	China	-0.2	-0.9	-0.5	-0.4
	India	0	0	0.5	1.7
	USA	0	0	-1.3	-3.5
	EU27+UK	0	0	-1.3	-3.5
	Russia	0	-0.6	-0.9	-1.5
	Japan	0	-0.3	-1.3	-3.6
	Brazil	0	0	-0.6	-2.2
NOx		January	February	March	April
	Global	-1.9	-10.6	-17.4	-30.4
	China	-7.5	-36.5	-17.6	-12.3
	India	0	0.2	-14.7	-41
	USA	-0.1	-1.1	-13.6	-36.2
	EU27+UK	-0.1	-1.1	-13.6	-36.2
	Russia	0	-7.3	-16.3	-35.6
	Japan	-0.1	-2	-9.1	-28.5
	Brazil	0	-0.3	-12.4	-35.7

Table S2. Comparison of fossil fuel CO_2 emission reduction (in percent) for the first quarter of 2020 from this study compared with other studies

	This study (%)	**High Le Quéré et al (%)**	**Mid Le Quéré et al (%)**	**Liu et al. (2020)[1] (%)**
Global	-8.50	-10.47	-6.30	-5.8
China	-15.97	-15.97	-10.00	-10.3
India	-5.07	-10.97	-6.07	-1.6
USA	-4.70	-10.87	-6.10	-4.20
EU27+UK	-4.70	-10.87	-6.10	-4.30
Russia	-7.23	-7.23	-4.00	-3.00
Japan	-2.43	-6.70	-3.40	-4.30
Brazil	-4.83	-6.10	-4.20	-4.10

Table S3. Comparison of monthly and annual CO_2 trends with Le Quéré et al (2020)

This Study		January	February	March	April	Annual
	Glob	-1.7	-9.2	-14.6	-27.5	-16.5
	CHN	-6.1	-29.4	-12.4	-7.9	-8.1
	IND	-0.1	0	-15.1	-41.7	-23.2
	USA	-0.1	-1.1	-12.9	-35.2	-19.6
	EU27+UK	-0.1	-1.1	-12.9	-35.2	-19.6
	RUS	0	-6.8	-14.9	-31.8	-18.3
	JPN	-0.1	-1.2	-6	-25	-13.8
	BRA	0	-0.4	-14.1	-39.4	-21.8
High Le Quere		January	February	March	April	Annual
	Glob	-2.2	-12.7	-16.5	-25.6	-13.3
	CHN	-6.1	-29.4	-12.4	-7.9	-9.8
	IND	-4.1	-9	-19.8	-35.9	-15.6
	USA	-0.4	-12.7	-19.5	-41.5	-18.8
	EU27+UK	-0.4	-12.7	-19.5	-41.5	-18.8
	RUS	0	-6.8	-14.9	-31.8	-12.7
	JPN	-1.1	-8.4	-10.6	-34	-14.4
	BRA	0	0	-18.3	-34.8	-17.7
Mid Le Quere		January	February	March	April	Annual
	Glob	-1.1	-7.6	-10.2	-17.5	-7.8
	CHN	-3	-19.5	-7.5	-4	-5.4
	IND	-2	-4.5	-11.7	-25.5	-8.7
	USA	-0.2	-6.2	-11.9	-30.3	-11.7
	EU27+UK	-0.2	-6.2	-11.9	-30.3	-11.7
	RUS	0	-3.3	-8.7	-22.4	-7.3
	JPN	-0.5	-4.2	-5.5	-23.3	-8.2
	BRA	0	0	-12.6	-24.6	-10.9

Table S4. Geoffory et al. (2013)[39,40] two layer model fits to CMIP6 model 4xCO_2 integrations

Model	Climate feedback parameter	Ocean layer heat exchange coefficient	Efficacy of deep ocean heat uptake	Ocean mixed layer heat capacity	Deep ocean heat capacity
	$Wm^{-2}K^{-1}$	$W\ m^{-2}\ K^{-1}$	-	$W\ yr\ m^{-2}\ K^{-1}$	$W\ yr\ m^{-2}\ K^{-1}$
ACCESS-CM2	-0.70	0.54	1.50	8.71	93.23
ACCESS-ESM1-5	-0.71	0.62	1.60	8.38	95.36
AWI-CM-1-1-MR	-1.21	0.48	1.45	8.20	56.49
BCC-CSM2-MR	-1.14	0.87	1.30	5.94	64.57
BCC-ESM1	-0.89	0.53	1.37	8.70	97.66
CAMS-CSM1-0	-1.92	0.48	1.28	9.75	56.97
CESM2	-0.66	0.67	1.77	8.41	75.91
CESM2-FV2	-0.58	0.71	1.77	7.42	92.73
CESM2-WACCM	-0.71	0.70	1.53	8.29	89.67
CESM2-WACCM-FV2	-0.60	0.70	1.50	8.17	112.10
CNRM-CM6-1	-0.75	0.51	0.99	7.59	145.23
CNRM-CM6-1-HR	-0.94	0.55	0.75	8.41	96.37
CNRM-ESM2-1	-0.63	0.60	0.90	7.47	97.02
CanESM5	-0.65	0.53	1.06	8.23	80.72
E3SM-1-0	-0.63	0.36	1.46	8.39	43.90
FGOALS-f3-L	-1.50	0.59	1.62	8.99	79.35
FGOALS-g3	-1.28	0.64	1.37	8.13	98.49
GFDL-CM4	-0.82	0.58	1.64	7.53	94.14
GFDL-ESM4	-1.46	0.55	0.86	8.37	148.07
GISS-E2-1-G	-1.50	0.84	1.11	7.54	140.89
GISS-E2-1-H	-1.14	0.62	1.12	8.64	84.25
GISS-E2-2-G	-1.64	0.53	0.65	8.89	411.85
HadGEM3-GC31-LL	-0.62	0.52	1.19	7.96	76.42
HadGEM3-GC31-MM	-0.65	0.59	1.00	8.24	71.42
IITM-ESM	-1.94	0.70	1.15	9.34	174.11
INM-CM5-0	-1.61	0.48	1.30	8.64	47.65
IPSL-CM6A-LR	-0.69	0.39	1.58	8.00	94.99
MIROC-ES2L	-1.56	0.68	0.95	10.59	177.43
MIROC6	-1.42	0.62	1.26	9.17	205.68
MPI-ESM1-2-HR	-1.27	0.64	1.40	8.41	92.63
MRI-ESM2-0	-1.20	0.86	1.48	8.48	98.20
NorESM2-LM	-0.93	0.82	3.07	5.60	145.05
NorESM2-MM	-1.54	0.77	1.69	6.15	121.29
SAM0-UNICON	-1.03	0.81	1.14	6.58	100.49
UKESM1-0-LL	-0.66	0.53	1.13	7.74	76.55

Table S5. Monthly surface ozone concentration (ppb) change estimates using the Turnock et al (2018)[28] parameterization averaged across different world regions.

Month	Central America	Central Asia	East Asia	Europe	Middle East	North Africa	North America	North Pole	Ocean	Pacific, Aus, NZ	Russia, Belarus, Ukraine	Southern Africa	South America	South Asia	South East Asia	South Pole	Global
Jan	-0.05	-0.06	-0.04	-0.06	-0.06	-0.07	-0.08	-0.07	-0.04	-0.01	-0.05	-0.02	-0.01	-0.05	-0.08	0.00	-0.04
Feb	-0.36	-0.45	-0.58	-0.47	-0.54	-0.53	-0.56	-0.45	-0.33	-0.09	-0.34	-0.15	-0.07	-0.37	-0.50	-0.03	-0.33
Mar	-1.05	-1.46	-1.46	-0.94	-1.98	-1.46	-1.20	-0.97	-0.79	-0.28	-0.95	-0.40	-0.38	-2.15	-1.10	-0.15	-0.81
Apr	-2.28	-2.91	-2.82	-2.51	-3.66	-2.74	-2.95	-2.13	-1.55	-0.68	-2.42	-0.74	-0.93	-4.75	-2.20	-0.37	-1.65
May	-1.42	-2.03	-1.75	-1.86	-2.64	-1.71	-2.02	-1.41	-0.96	-0.40	-1.61	-0.44	-0.54	-2.83	-1.40	-0.28	-1.05
Jun	-1.35	-1.81	-1.55	-1.83	-2.93	-1.51	-1.92	-1.00	-0.90	-0.41	-1.37	-0.48	-0.53	-2.43	-1.37	-0.32	-0.97
Jul	-1.28	-1.43	-1.29	-1.84	-2.68	-1.32	-1.94	-0.65	-0.90	-0.45	-1.18	-0.49	-0.55	-2.08	-1.34	-0.36	-0.93
Aug	-1.29	-1.42	-1.29	-1.62	-2.62	-1.24	-1.80	-0.57	-0.89	-0.50	-1.06	-0.47	-0.57	-2.19	-1.35	-0.39	-0.91
Sep	-1.27	-1.38	-1.37	-1.37	-2.65	-1.30	-1.61	-0.74	-0.87	-0.56	-0.97	-0.49	-0.57	-2.71	-1.39	-0.40	-0.91
Oct	-1.41	-1.29	-1.37	-0.92	-2.64	-1.56	-1.26	-0.94	-0.89	-0.54	-0.72	-0.50	-0.60	-3.20	-1.42	-0.36	-0.92
Nov	-1.37	-0.89	-1.20	-0.53	-2.03	-1.46	-0.90	-0.90	-0.93	-0.52	-0.48	-0.57	-0.63	-3.03	-1.58	-0.31	-0.90
Dec	-1.28	-0.75	-1.09	-0.10	-1.45	-1.35	-0.56	-0.72	-0.87	-0.47	-0.19	-0.61	-0.57	-2.57	-1.43	-0.26	-0.81
Annual Mean	**-1.20**	**-1.32**	**-1.32**	**-1.17**	**-2.16**	**-1.35**	**-1.40**	**-0.88**	**-0.83**	**-0.41**	**-0.95**	**-0.45**	**-0.50**	**-2.36**	**-1.26**	**-0.27**	**-0.85**